

## New TRPM8 modulators induce melanoma cell death

Lauretta C.<sup>1</sup>, Sorrentino C.<sup>1</sup>, D'Angiolo R.<sup>1</sup>, De Rosa J.<sup>1</sup>, Smaldone G.<sup>2</sup>, Ciaglia T.<sup>2</sup>, Musella S.<sup>2</sup>, Bertamino A.<sup>2</sup>, Giovannelli P.<sup>1</sup>, Migliaccio A.<sup>1</sup>, Castoria G.<sup>1</sup>, Di Donato M.<sup>1</sup><sup>1</sup>Department of Precision Medicine, School of Medicine, University of Campania 'L. Vanvitelli', Via L. De Crecchio 7, 80138, Naples, Italy.<sup>2</sup>Department of Pharmacy, University of Salerno, Via G. Paolo II, 84084, Fisciano, SA, Italy.

rosa.dangiolo@unicampania.it

## INTRODUCTION &amp; AIM

The global incidence of melanoma is rising steadily. Despite significant advancements in therapeutic options, resistance mechanisms often emerge, leading to disease progression. This event underscores the importance of identifying novel intracellular targets. The transient receptor potential melastatin subtype 8 (TRPM8), a non-selective cation channel with a preference for calcium permeation, is aberrantly expressed in various solid malignancies, including melanoma. Thus, it could represent a promising therapeutic target in melanoma cells.

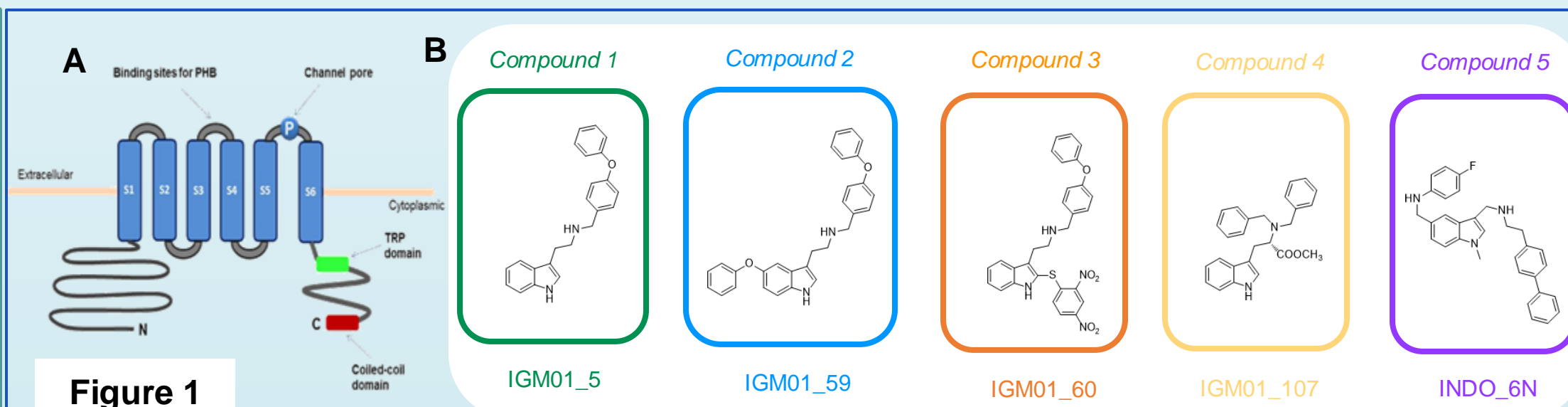


Figure 1

**Figure 1:** (A) Schematic diagram of TRPM8 structure. In (B), molecular structure of TRPM8 modulators tested in melanoma cells (described in Di Donato et al., 2019 Sci Rep).

## METHOD

Two melanoma cell lines, derived from subcutaneous and lymph node metastases, were utilized to investigate the effects of TRPM8 modulators. Multiple methodologies, including colorimetric assays, western blotting, immunofluorescence (IF), and confocal microscopy, were employed to assess the biological impact of these modulators.

## RESULTS &amp; DISCUSSION

Time-course experiments demonstrated that TRPM8 modulators induced melanoma cell death. These findings were corroborated by dual-fluorescence IF analyses. Further investigation of the molecular mechanisms revealed that the apoptotic pathway triggered by these modulators involved caspase 3 activation.

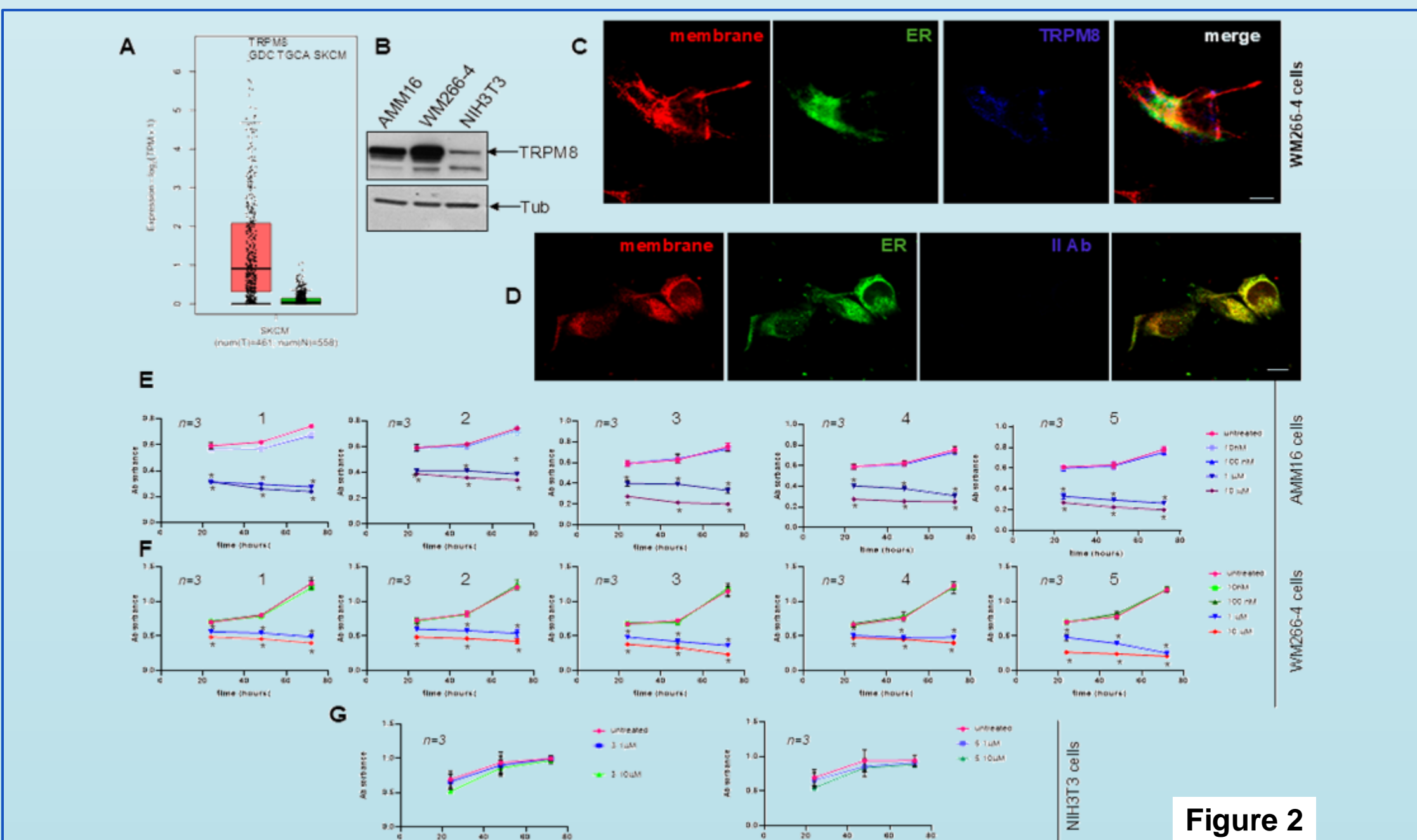


Figure 2

**Fig 2:** In (A) TRPM8 expression levels in melanoma specimens and in normal tissues (n = 1019). TRPM8 was higher expressed in tumors (red; n = 461) than in normal counterparts (green; n = 558). In (B), Western blotting (WB) analysis for TRPM8 expression. In (C), plasma membrane (red), endoplasmic reticulum (green), and TRPM8 channel (blue) were stained and analyzed by Immunofluorescence (IF). Scale bar, 10µm. The specificity of the IF approach was shown in the control staining (D). AMM16 (E), WM2664 (F) and NIH3T3 (G) cells were left untreated or treated as indicated. Cell viability was assayed using the WST-8 reagent. Experiments were performed in triplicate (n=3). \*: p < 0,05.

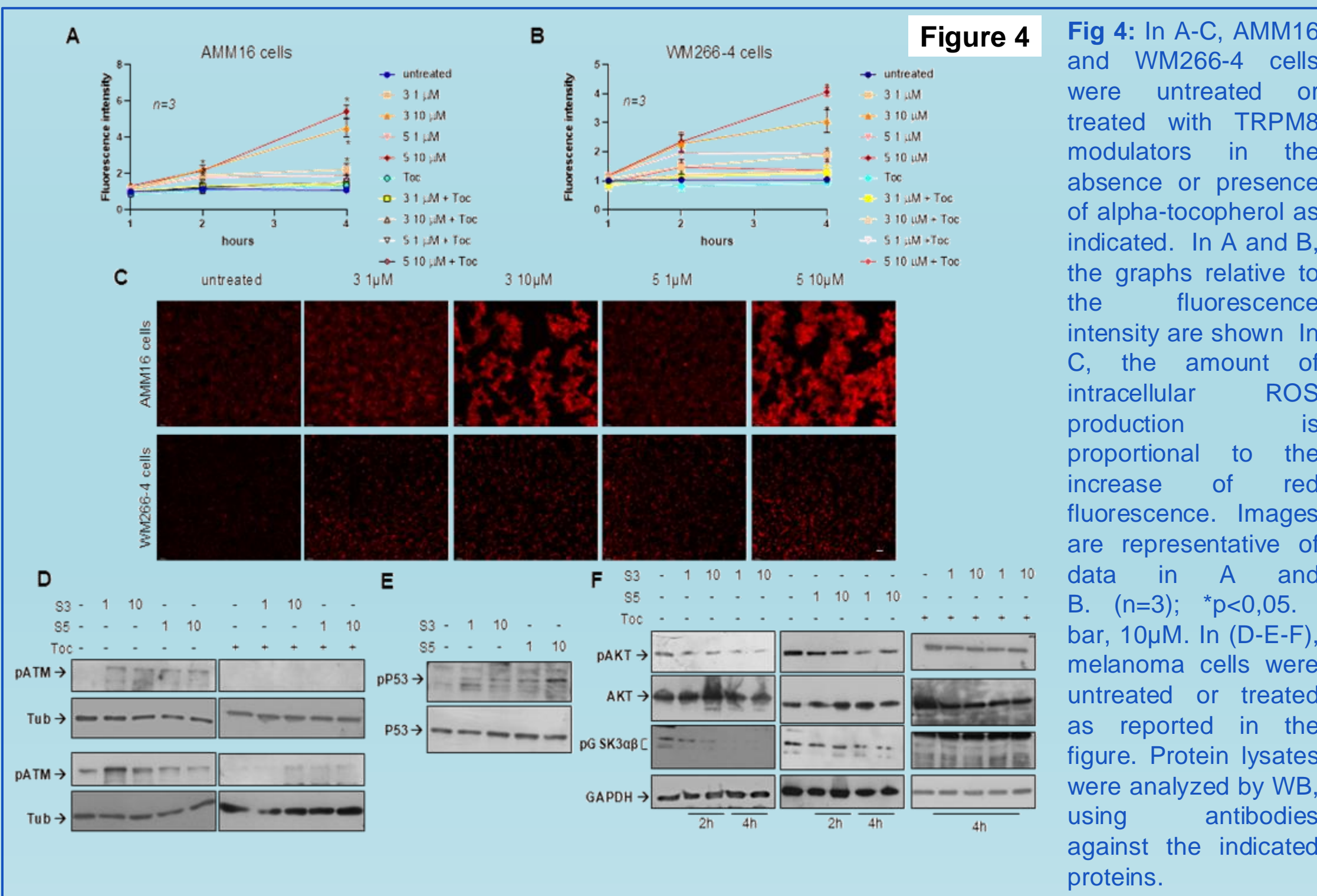


Figure 4

**Fig 4:** In A-C, AMM16 and WM266-4 cells were untreated or treated with TRPM8 modulators in the absence or presence of alpha-tocopherol as indicated. In A and B, the graphs relative to the fluorescence intensity are shown. In C, the amount of intracellular ROS production is proportional to the increase of red fluorescence. Images are representative of data in A and B. (n=3); \*p<0,05. bar, 10µm. In (D-E-F), melanoma cells were untreated or treated as reported in the figure. Protein lysates were analyzed by WB, using antibodies against the indicated proteins.

## CONCLUSION

Additional studies are necessary to elucidate the regulatory mechanisms of TRPM8 and the resulting calcium influx dynamics. Nonetheless, the identification of novel chemotherapeutic targets with enhanced potency and selectivity may pave the way for innovative melanoma treatment strategies. These approaches hold significant promise for advancing oncology therapeutics.

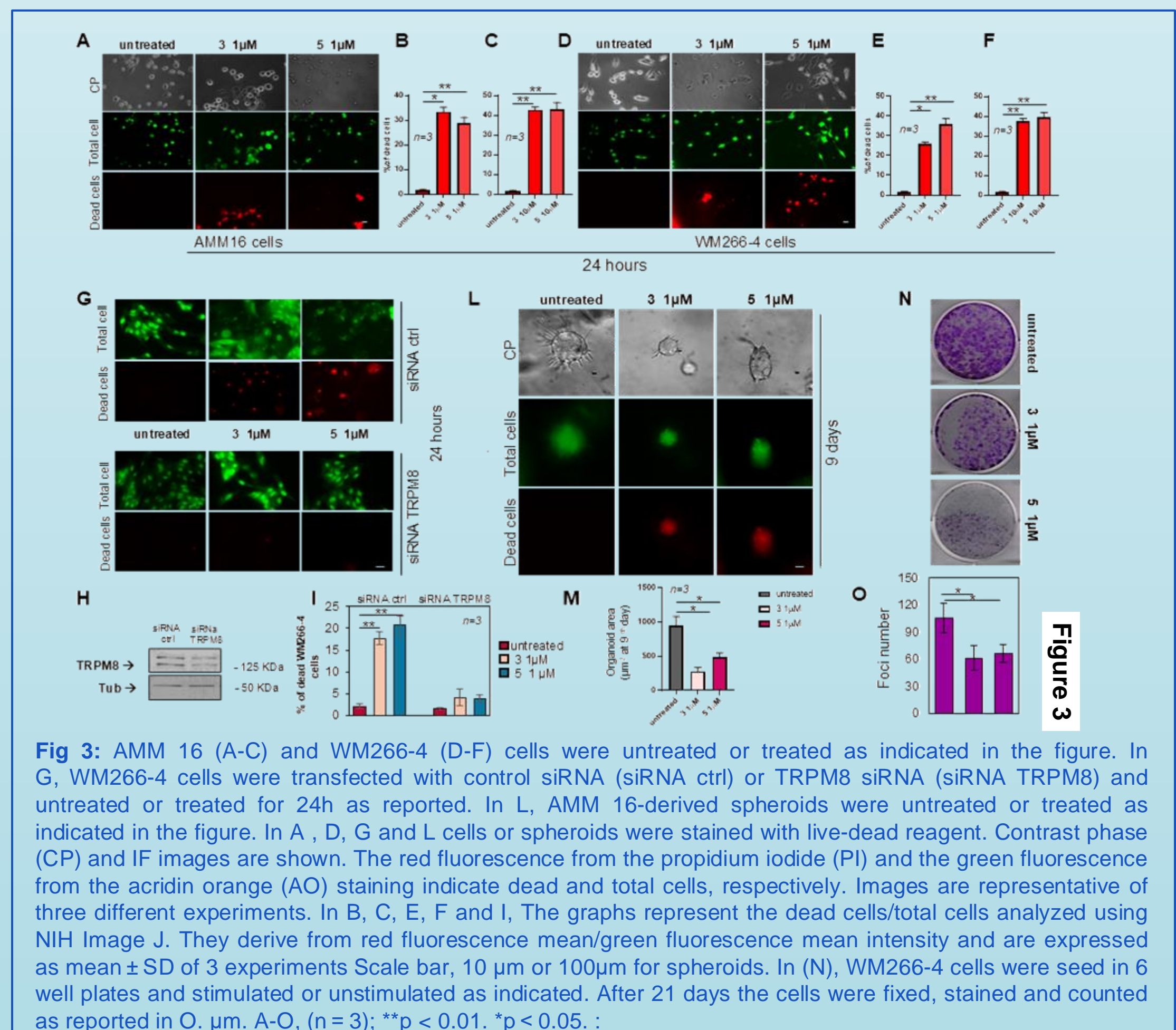


Figure 3

**Fig 3:** AMM 16 (A-C) and WM266-4 (D-F) cells were untreated or treated as indicated in the figure. In G, WM266-4 cells were transfected with control siRNA (siRNA ctrl) or TRPM8 siRNA (siRNA TRPM8) and untreated or treated for 24h as reported. In L, AMM 16-derived spheroids were untreated or treated as indicated in the figure. In A, D, G and L cells or spheroids were stained with live-dead reagent. Contrast phase (CP) and IF images are shown. The red fluorescence from the propidium iodide (PI) and the green fluorescence from the acridin orange (AO) staining indicate dead and total cells, respectively. Images are representative of three different experiments. In B, C, E, F and I, The graphs represent the dead cells/total cells analyzed using NIH Image J. They derive from red fluorescence mean/green fluorescence mean intensity and are expressed as mean ± SD of 3 experiments Scale bar, 10 µm or 100µm for spheroids. In (N), WM266-4 cells were seed in 6 well plates and stimulated or unstimulated as indicated. After 21 days the cells were fixed, stained and counted as reported in O. µm. A-O, (n = 3); \*\*p < 0.01. \*p < 0.05. :

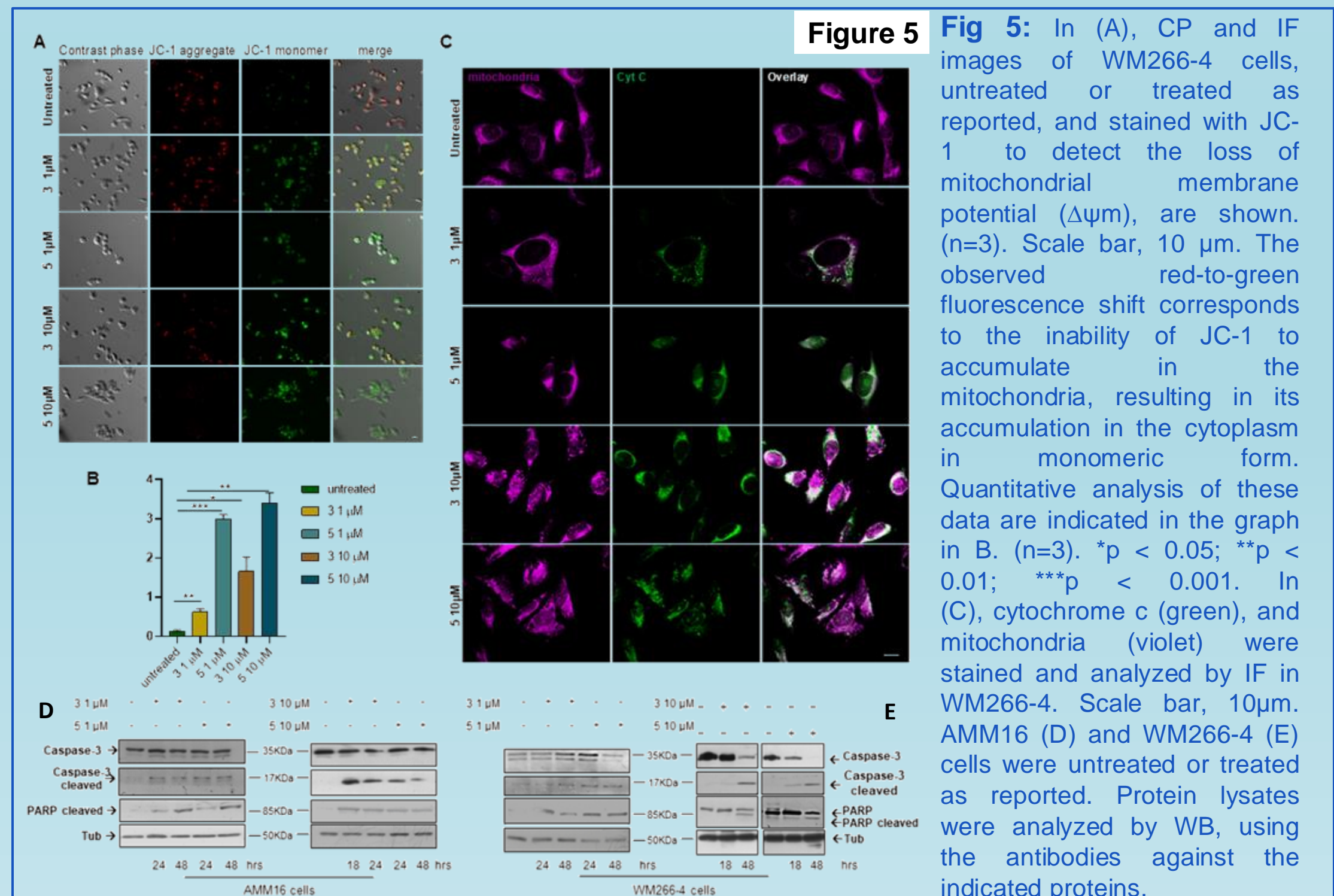


Figure 5

**Fig 5:** In (A), CP and IF images of WM266-4 cells, untreated or treated as reported, and stained with JC-1 to detect the loss of mitochondrial membrane potential ( $\Delta\psi_m$ ), are shown. (n=3). Scale bar, 10 µm. The observed red-to-green fluorescence shift corresponds to the inability of JC-1 to accumulate in the mitochondria, resulting in its accumulation in the cytoplasm in monomeric form. Quantitative analysis of these data are indicated in the graph in B. (n=3). \*p < 0.05; \*\*p < 0.01; \*\*\*p < 0.001. In (C), cytochrome c (green), and mitochondria (violet) were stained and analyzed by IF in WM266-4. Scale bar, 10µm. AMM16 (D) and WM266-4 (E) cells were untreated or treated as reported. Protein lysates were analyzed by WB, using the antibodies against the indicated proteins.